Rain and Dust: Magnetic Records of Climate and Pollution

The alternating light-coloured loess layers and reddish brown palaeosols, revealed in the walls of erosional gullies, provide a stunning visual record of past changes in the strength of the East Asian summer and winter monsoons.

Barbara A. Maher*

1811-5209/09/0005-0229$2.50 DOI: 10.2113/gselements.5.4.229

Two contrasting examples of the application of mineral magnetism to environmental problems are discussed. Magnetic susceptibility measurements of sediments from the Chinese Loess Plateau – the biggest accumulation of windblown sediments on Earth – reveal one of the best records of continental climate change available. These records provide a detailed picture of glacial and interglacial cycles and variations in the East Asian summer monsoon stretching back more than 2 million years. In the case of anthropogenic airborne particles, the spread of particulate pollutants can be robustly traced throughout a city environment by measuring the magnetic properties of leaves, which trap magnetic particles released from vehicle exhausts and/or industry emissions.

KEYWORDS: magnetic susceptibility, climate change, summer monsoon, particulate pollution, health impacts

MAGNETIC RECORDS OF PAST CLIMATE

What Is Loess?

To obtain long records of past climate change from sediments, we look at sites far away from past or present glaciers, where layers of sediment have accumulated without disturbance for hundreds of thousands of years. Such sites include the deep-sea floor and, on land, the famous Loess Plateau of north-central China (FIG. 1). These thick, extensive deposits of windblown dust (loess) have been the subject of intense scientific attention over the last ~20 years. The loess spans at least the last ~2 million years (My) of Earth's history, preserving the longest, most detailed record of Quaternary climatic changes yet found on land. Covering some 440,000 km^2 and comprising ~2 × 10^5 km^3 in volume (comparable with, say, the volume of the mountains of Scandinavia), the Chinese loess forms a vast wedge of sediment, thickest (~350 m) near the eastern edges of Mongolia and Tibet, about 150 m thick in the central area, and thinning out towards the south and east. Around Xi'an, for example (the home of the famous Terracotta Army, which is also made of loess!), the loess sediment pile is ~150 m in thickness.

The loess accreted upwards quasi-continuously, as aeolian dust blown from the western deserts and uplands. It was deposited onto the land surface to the east and south, successively burying previously deposited dust, a process proceeding for >2 My. The loess comprises an extremely homogenous, slightly cemented mix of quartz (~35%), phyllosilicates (~25%), plagioclase (10–15%), calcite (~10–15%), K-feldspar (~5%), dolomite and amphibole (≤ 5%), together, critically, with minor amounts of hematite and goethite and trace amounts of magnetite and maghemite.

* Centre for Environmental Magnetism and Palaeomagnetism
Lancaster Environment Centre, University of Lancaster
Lancaster, LA1 4YQ, UK
E-mail: b.maher@lancaster.ac.uk

How Does Loess Record Past Climate?

The fate of the dust once deposited on the land surface has depended on the intensity of the two East Asian monsoon systems. During glacial climate stages, when the winter monsoon was intense and cold, dry, dusty winds were blowing from the inner Asian continent towards the Pacific (FIG. 1), the rate of loess deposition was higher, and previously deposited loess was rapidly buried by more loess. During interglacial stages, when the summer monsoon was strong and warm, moisture-laden air was blowing from the Pacific across China, the land surface became more vegetated and the loess was increasingly weathered to form a surficial layer of soil. At these times, dust accumulation did not cease, but the dustfall tended to be finer and deposition rates were often slower. In the thicker loess sequences, there are >35 'fossil' soils (palaeosols) interbedded with less-weathered loess units (INSET); the major soil units are traceable across the Loess Plateau for hundreds of kilometres. The glacial/interglacial alternations between the pale, buff-coloured loess layers and the reddish brown palaeosols form a dramatic, visual record of the waxing and waning of the winter and summer monsoon systems through the Quaternary geological period.

FIGURE 1 The East Asian monsoon systems

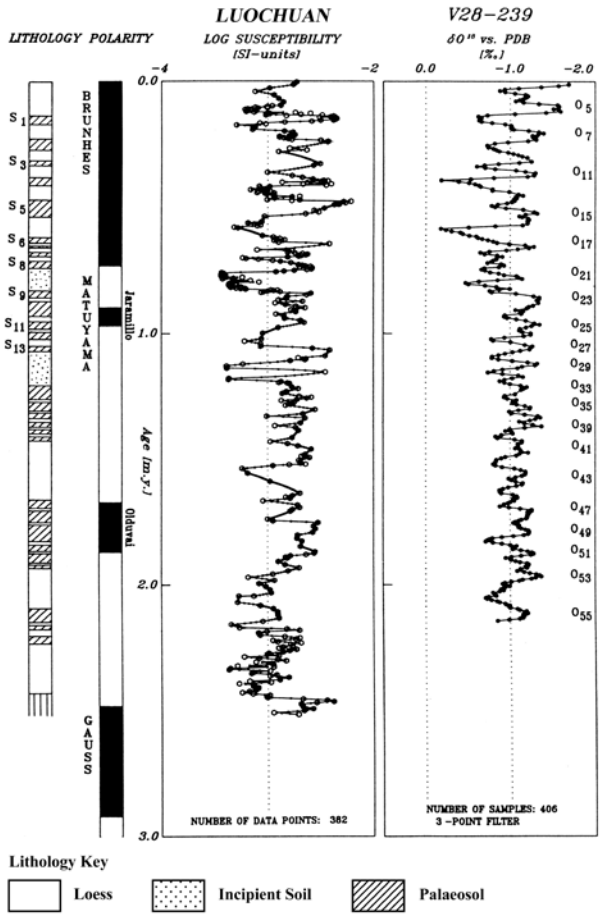

FIGURE 2 Left to right: loess/palaeosol stratigraphy at Luochuan (central Plateau) (S1–S13 = palaeosol 1 to palaeosol 13); palaeomagnetic stratigraphy and dating (black = period of normal polarity; white = reverse polarity); magnetic susceptibility; deep-sea oxygen isotope record (O_n = oxygen isotope stage, odd numbers = interglacials). FROM HELLER AND LIU (1986)

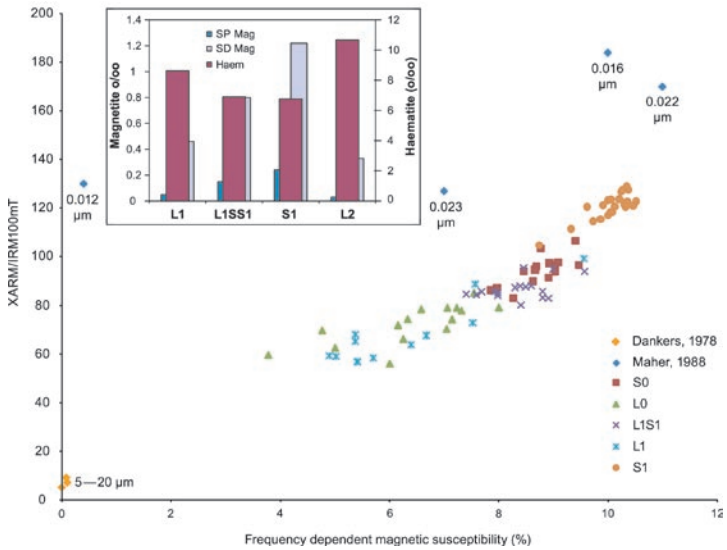

FIGURE 3 χ_{ARM}/IRM_{100mT} versus frequency-dependent susceptibility for samples of loess and palaeosol, central Loess Plateau, and, for comparison, magnetite powders of known grain size. Compared with the χ_{ARM}/IRM values for the pure, grain-sized magnetite, the loess and palaeosols show some offset, because they also contain some hematite/goethite. Inset: mathematical unmixing of the magnetic minerals and grain sizes in loess unit 1 (L_1), an incipient soil within L1 (L_1SS_1), the last interglacial palaeosol (S_1), and loess unit 2 (L_2) (Maher and Thompson 1992)

Given the prospect of future changes in monsoonal rainfall in this densely populated region, retrieval of quantitative data regarding past climates from these natural archives is an important task. The vertical sequences of loess/palaeosols within the Loess Plateau carry a detailed magnetic record of both time and climatic change. First, the sediments record all six major polarity reversals of the Earth's magnetic field during the last 2.5 My, thus providing a firm basic chronology (FIG. 2; Heller and Liu 1986). Second, compared to the loess, the Chinese palaeosols contain higher (but still trace) concentrations of strongly magnetic iron oxides (comprising a mix of minerals spanning the magnetite–maghemite solid solution series) of distinctively ultrafine grain size (≤0.05 micrometre in diameter). The less weathered loess layers contain much smaller concentrations of this distinctive magnetic material. These differences can be easily and rapidly quantified by measuring magnetic susceptibility; the susceptibility of the palaeosols is always higher than that of the less weathered loess units. Palaeosols in the presently semi-arid western Plateau display the lowest susceptibility values; palaeosols in the more humid central and southern Plateau display increasingly higher magnetic susceptibility values. For the loess layers, the lowest 'background' magnetic susceptibility (~20–30 × 10^{-8} m^3 kg^{-1}) is seen in the thickest sequences, i.e. where the loess deposition rate was highest and the degree of post-depositional weathering least.

The global significance of these magnetic susceptibility variations can be seen when they are compared with the Quaternary record of marine oxygen isotope changes. During past glacial stages, continental-scale ice sheets 'locked up' significant quantities of isotopically light oxygen (^{16}O), leaving the world's oceans proportionally enriched in isotopically heavy oxygen (^{18}O). These ocean isotopic shifts are recorded in the calcium carbonate skeletons of marine micro-organisms (foraminifera). Strong correlation is evident between the loess/palaeosol magnetic susceptibility and the deep-sea oxygen isotope record (FIG. 2), indicating coupling of the Asian monsoon systems with the Earth's intensifying global cycles of glaciation and deglaciation, especially between ~0.75 Ma and the present.

Magnetic Contrasts between Loess and Palaeosols

The magnetic minerals of the Chinese loess and palaeosols have been identified and quantified by applying a range of magnetic measurement techniques. These methods rapidly and easily discriminate changes in mineralogy and grain size, even at minor and trace concentrations (well below the detection level of X-ray powder diffraction, for example). Present in both the parent loess and the palaeosols are the ferrimagnetic iron oxides (ferrites) magnetite and maghemite (and intermediaries along the solid solution between them), and the weakly magnetic iron oxide hematite and oxyhydroxide goethite. The soils are significantly more magnetic than the loess, but both display steep rises in magnetic remanence at low applied fields (up to ~0.1 T), indicative of ferrimagnetic behaviour. Both also acquire some remanence at high fields (>0.2 T); the high-coercivity minerals contribute ~6% of the loess saturation remanence and even less, ~2.5%, in the palaeosols. However, given their much weaker magnetic properties, these values indicate that hematite/goethite are ~10 times more abundant than magnetite/maghemite in these oxic loess and soil layers. The presence of magnetite is confirmed by thermomagnetic measurements; it occurs along with variable amounts of maghemite, some of which oxidizes during heating in air (at ~400°C) to hematite. Both loess and palaeosols from the drier western Plateau contain more maghemite than the sediments from the south and central Plateau.

The colour of the palaeosols gives an immediate clue that the original detrital iron oxide assemblages in the loess underwent significant transformation and grain size changes during weathering; their reddish soil hues reflect in situ, pedogenic formation of very fine-grained (≤25 nm) goethite and hematite. That the grain size of ferrites in the palaeosols is also much finer than in the parent loess is evident from measurements of frequency-dependent susceptibility, low-temperature susceptibility and anhysteretic remanence (see Glossary on page 215). The palaeosols display decreasing magnetic susceptibility with increased measurement frequency (e.g. measured at 0.47 kHz and 4.7 kHz) and with lowered temperature, indicating ferrite grains which are superparamagnetic (SP) at room temperature/lower measurement frequency. Decreasing temperature and increasing frequency cause some SP grains to 'block in' and act as single-domain (SD) grains, with lower susceptibilities (~10–15% lower in the palaeosols here). Another grain size–sensitive magnetic parameter is anhysteretic remanence (χ_{ARM}), which peaks for ferrites close to the SP/SD size boundary (~0.03 μm). Combining frequency-dependent susceptibility data with χ_{ARM}/SIRM (saturation remanence) ratios for the loess and palaeosols, and, for comparison, magnetite grains of known size, the least weathered loesses plot towards the coarse-grained, multi-domain (MD) magnetite grains of ≥5 μm diametre; the most developed soils plot towards the SP/SD size range (Fig. 3). Using the remanence and susceptibility data, the magnetic mineralogy of the Chinese loess and palaeosols can be quantitatively unmixed (Fig. 3 inset, Maher and Thompson 1992; Liu et al. 2004). The palaeosols are more magnetic compared with their parent loess because they contain more SP (~0.3‰) and SD (~1.2‰) ferrimagnets and slightly less hematite/goethite (~6‰). By concentrating the magnetic minerals using magnetic extraction techniques, we can use methods such as electron microscopy to confirm the mineralogy (Fig. 4).

Having accounted for why magnetic susceptibility behaves this way in the Chinese loess/palaeosol sequences, can we use it to make quantitative estimates of palaeoclimatic changes, in order, for example, to test the validity of numerical climate simulations run not for the future but the past? Studies of modern soils provide very useful information with which to interpret the palaeosols. In modern soils, ultrafine-grained magnetite/maghemite is formed in situ in well-drained soils of near-neutral pH (~6–8), developing on iron-bearing, weatherable parent materials. In more acidic or permanently wet soils, such ferrites do not form or are reduced to non-magnetic forms (also true for palaeosols which underwent such conditions, e.g. some palaeosols in the Alaskan loess). Measurements of modern soils across the Chinese Loess Plateau and other independent sites, including the loess-mantled Russian steppe (Maher et al. 2002), show that the amount of magnetic material formed (as measured by magnetic susceptibility) is strongly and positively correlated with annual rainfall (Fig. 5). New, ultrafine-grained ferrites can form in soils when iron is supplied in its reduced (Fe^{2+}) form, through the action of iron-reducing bacteria. Upon wetting, parts of the soil micro-environment become oxygen poor. The iron-reducing bacteria then become active (they use iron rather than oxygen in their metabolism) and release Fe^{2+} into the soil matrix where it may, on drying or re-oxidation of the soil, react with Fe^{3+} oxides to form magnetite. The grain size distribution of the pedogenic magnetite, notably similar across modern soils and palaeosols, reflects its extracellular precipitation under those pH, Eh and Fe supply conditions that 'suit' the bacteria. Such bacterial activity will be greater in soils which undergo more frequent wetting and drying cycles. These pathways of pedogenic magnetite formation can thus account for the strong positive correlation between rainfall and soil-formed magnetic susceptibility.

Retrieving Quantitative Estimates of Past Rainfall from Magnetic Susceptibility Measurements

For the Chinese loess/palaeosol sequences, with their well-drained, near-neutral soils, we can use the magnetic susceptibility/rainfall relationship from modern soils (Fig. 5) to calculate past rainfall (palaeorainfall) from the magnetic susceptibility of the palaeosols. By measuring susceptibility at many Plateau locations, it is possible to map rainfall patterns at different climate stages. Compared to the present day, there was higher rainfall (more intense summer

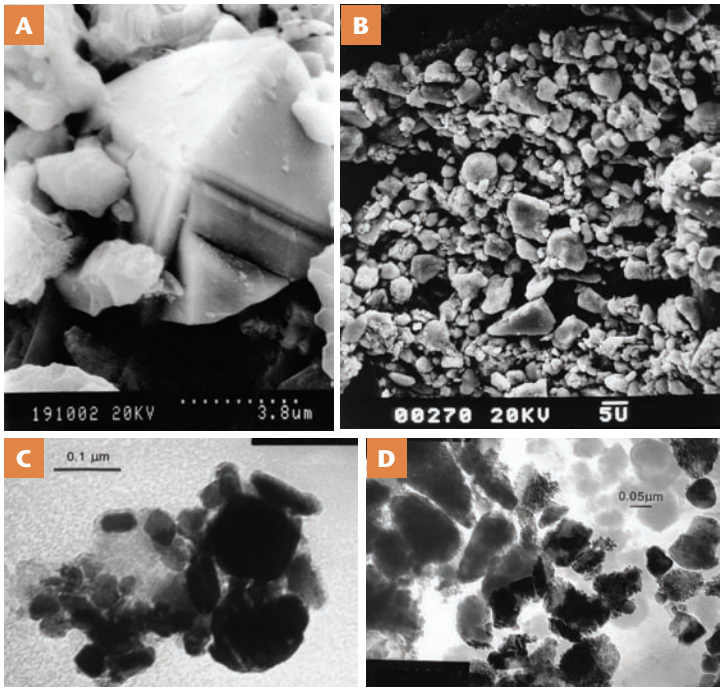

Figure 4 Scanning (A, B) and transmission (C, D) electron micrographs of (**A**) detrital, lithogenic titanomagnetite grain from loess; (**B**) a collection of lithogenic magnetite grains from loess; (**C**) and (**D**) pedogenic, ultrafine-grained ferrites (magnetite–maghemite intermediaries) from palaeosol, Luochuan. Photos by B.A. Maher

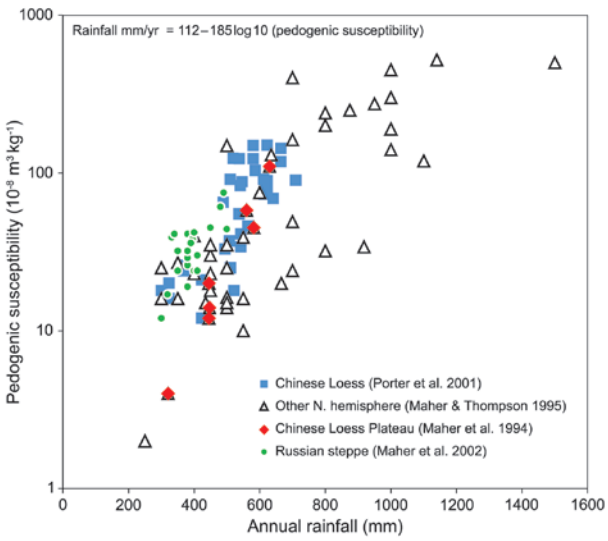

Figure 5 Relationship between pedogenic (soil-formed) magnetic susceptibility and annual rainfall for modern loessic soils and modern (last 30-year averages) rainfall. Statistical examination of the relationships between the soil magnetic properties and major climate variables (temperature, rainfall, etc.) identifies annual rainfall as the most significant factor ($R^2 = 0.88$). The relationship between soil magnetism and rainfall can thus be expressed as the equation shown in the figure. From Maher et al. 2002

monsoons) in the early Holocene (about 6–8 ky before present, BP). During the last glaciation (around 20 ky BP), rainfall was reduced across the whole region, while in the last interglacial (~120–125 ky BP), rainfall was much higher especially in the western Plateau, which is semi-arid at present. Additionally, we can estimate rainfall changes through time at any one location, whether for the last ten thousand (Fig. 6A) or last one million years or more (Fig. 6B). Other rainfall proxies, such as the concentration of beryllium-10 in the sediments (^{10}Be, produced in the upper atmosphere by cosmic bombardment, is washed out by rainfall; e.g. Sartori et al. 2005) or stable isotope fractionation in organic matter (e.g. Ning et al. 2008), substantiate the magnetism/climate relationship. However, such techniques are much more expensive and time-consuming and so have yet to be applied at the scale of the powerful magnetic proxy.

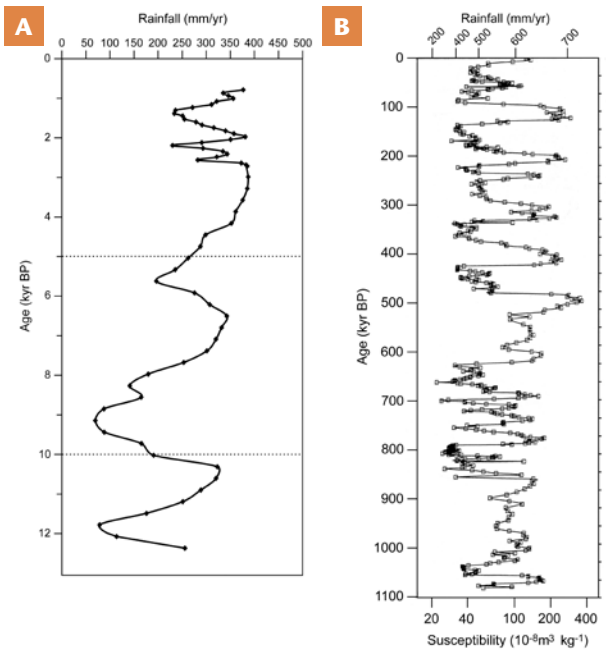

Figure 6 Palaeorainfall estimated from the magnetic susceptibility/rainfall climofunction for (**A**) the last 10,000 years (Duowa, western Loess Plateau) and (**B**) the last 1.1 million years (Xifeng, central Plateau). From Maher and Thompson (1995) and Maher (2008)

MAGNETIC TRACING OF PARTICULATE POLLUTION

Human Health and Exposure Measurement Problem

Particulate matter is the most harmful pollution component widely present in the environment (Donaldson 2003), with no known level at which adverse health effects do not occur (Bealey et al. 2007). The presence of airborne pollutant particles (particulate matter, PM) below 10 μm in size (PM_{10}), especially those below 0.1 μm ($PM_{0.1}$), is of current concern due to adverse health effects associated with their inhalation (e.g. Morris et al. 1995; Pope et al. 2002; Calderón-Garcidueñas et al. 2008).

Worldwide, it is estimated that fine-grained PM ($PM_{2.5}$) causes 3% of mortality from cardio-pulmonary disease; 5% of mortality from cancer of the trachea, bronchus and lung; and 10% of mortality from acute respiratory infections in children under five (Cohen et al. 2005). It is currently estimated that the increases in overall mortality, cardiovascular mortality, and lung cancer mortality are 4%, 6% and 8%, respectively, per 10 μg/m^3 of PM_{10}. In extremely polluted urban environments (e.g. Mexico City), evidence indicates that ultrafine particle exposure is involved in the very early onset of Alzheimer's and Parkinson's diseases (Calderón-Garcidueñas et al. 2008). Fine particles (e.g. <1 μm), especially those containing metals such as Fe and Pb, which are often associated with organic carcinogens (including polyaromatic hydrocarbons – PAHs), may be the most damaging to health. Such fine grains, comprising very large particle numbers (~10^6–10^9/μg), can be breathed deeply into the lungs, overwhelming the capacity of white blood cells to engulf and remove them and leading to prolonged tissue contact times and resultant inflammation. Their high surface area also enhances their potential bioavailability (Donaldson 2003). Interactions between Fe-rich particles and epithelial tissues may generate free radicals, leading to oxidative cell damage (Aust et al. 2002). However, analysis of causal links between particulate pollution and specific health impacts has been hampered by poor reliability of data on human exposure. Exposure assessments tend to be weak, typically available only at coarse spatial resolution. For example, for vehicle-derived pollutants, air quality monitoring networks are hampered by both sparse spatial coverage and the location of monitoring stations at sub-optimal roadside distances and/or heights above ground level. A new approach, **biomagnetic monitoring**, may provide a robust and cost-effective means to achieve measurement and sourcing of PM_{10} at unprecedented levels of spatial resolution and is applicable all around the world (e.g. Shu et al. 2001, in China; Gautam et al. 2005, in Nepal; Pandey et al. 2005, in India; Chaparro et al. 2006, in Argentina; Kim et al. 2007, in Korea; Szönyi et al. 2008, in Europe).

Magnetic Particles in Anthropogenic Pollution

Urban anthropogenic particulates are enriched in toxic trace metals (including Fe, Pb, Zn, Ba, Mn, Cd and Cr) and, almost invariably, magnetic particles. The latter derive from iron impurities in fuels, which upon combustion form a non-volatile residue, often a mix of ferrimagnetic (magnetite/maghemite-like) and imperfectly antiferromagnetic (hematite-like) iron oxides. These combustion-derived PM_{10} components can also be PAH rich (Halsall et al. 2008), forming a harmful pollution 'cocktail'. In urban dusts, a strong correlation has been observed between magnetic susceptibility/remanence and PM_{10} (Muxworthy et al. 2002; Halsall et al. 2008; Szönyi et al. 2008; Mitchell and Maher 2009), dust mass, and sample mutagenicity (e.g. Morris et al. 1995). Leaves from roadside trees form natural, widely distributed collection surfaces for pollutants (Fig. 8). They provide a large surface area for PM collection (Matzka and Maher 1999), are often widely distributed in urban areas, provide samples at pedestrian-relevant heights, and require no power source or protection. The leaves can be picked and their surface area can be quickly and easily measured by pixel counting of scanned images. The leaves can then be folded to fit inside plastic sample pots and analysed magnetically (Fig. 7), providing a quantitative proxy for PM_{10} concentrations and magnetic particle size, particularly from vehicle combustion sources (Matzka and Maher 1999; Mitchell and Maher 2009).

Figure 8A shows the spatial variation in saturation remanence (SIRM) of birch leaves from trees spanning the rural coast of Norfolk and its small, industry-free but heavily trafficked inland city Norwich (SE England). Leaves growing at the coast have very low SIRMs; increasingly high values are displayed by leaves with increasing proximity to the urban area roadside (Matzka and Maher 1999). Compared with a coastal site (leaf SIRM = 3 × 10^{-6} A), roadside SIRMs were ~22 times higher. For leaves sampled from the central reservation (median strip) of a major four-lane highway close to Norwich city centre, leaf area–normalised (2D)

SIRMs were always higher on the uphill-adjacent side of the sampled trees (Fig. 8b). For a similar size and type of city, Lancaster (NW England), leaves sampled in the city centre (Mitchell and Maher 2009) had a 2D SIRM of 332×10^{-6} A (>100 times 'background', also 3×10^{-6} A). To assess how well leaf magnetic values represent the PM_{10} concentrations in the air, pumped air samples (120 litres) were collected over one hour at peak traffic flow at each sampled Lancaster tree location (Mitchell and Maher 2009). The air filter SIRMs show strong positive correlation with the measured leaf SIRMs; in turn, the air filter SIRMs are strongly correlated with particulate mass, and thus the leaf SIRMs are strongly correlated with the ambient particulate concentrations (Fig. 8c).

For both cities, IRM acquisition experiments indicate magnetite is the dominant magnetic component of the pollutants. Upon thermal demagnetization of a low-temperature (77 K) SIRM, the Lancaster leaf samples all display some degree of remanence loss, at between 114 and 127 K. The variable remanence loss may indicate the additional presence of some maghemitised magnetite and/or some ultrafine (SP) particles (Özdemir et al. 1993). Comparing the leaf and air filter χ_{ARM}/SIRM ratios and median destructive field (MDF_{ARM}) values with those for magnetite grains of known size indicates the dominant grain size of the magnetic pollutants is between ~0.1 and 1 μm (Özdemir and Banerjee 1982; Maher 1988).

Scanning electron microscopy of the co-located leaf and pumped air particles shows pollutants concentrated along ridges in the leaf surface (Fig. 7), with many of the sub-micrometre particles comprising rounded spherules, in contrast to the larger particles, often more angular. Many of the sub-micrometre leaf and filter particles are Fe rich; the larger, more angular particles have higher concentrations of Al and Si. Particle size measurement (of the longest axes of 100 imaged particles) supports the magnetically determined grain size range of ~0–1 μm.

For the Norwich study, strong correlation was observed between leaf SIRMs and Fe and Pb, the latter a significant neurotoxin in children even at low concentrations. Leaf particulate Pb, Fe and SIRM concentrations show peak values at ~0.3 m and 1.5–2 m above ground level. In contrast, Zn, Ba and Mn display lowest values at 0.3 m, and they steadily increase in concentration with height, indicating a more pervasive distribution of these metals. The association between highest SIRM, Pb and Fe values on the uphill roadside shows that fuel combustion is the major pollutant source; these patterns would not arise from re-suspension of roadside dust (Filippelli et al. 2005), nor from tyre, brake or other vehicle wear. There is a stronger correlation between leaf SIRM and Pb values than between Pb and Fe, suggesting that the magnetic and Pb-bearing particles come from the same source, most likely fuel combustion. This present-day co-association of automotive Pb and magnetic Fe emissions is evident despite the introduction of unleaded petrol (1986 in the UK). Lead poses some health risk at any level of exposure, particularly with regard to brain and kidney damage, hearing impairment

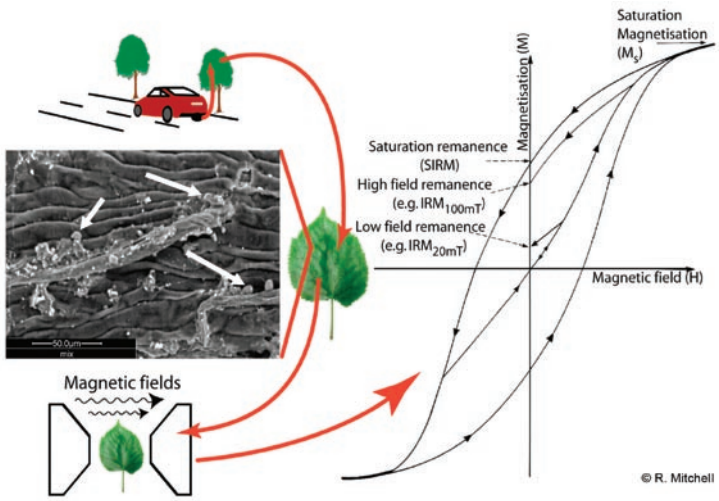

Figure 7 Sampling and measurement of roadside leaves as natural biomonitors of particulate pollution. Arrows on SEM image of leaf show spherules (Mitchell and Maher 2009)

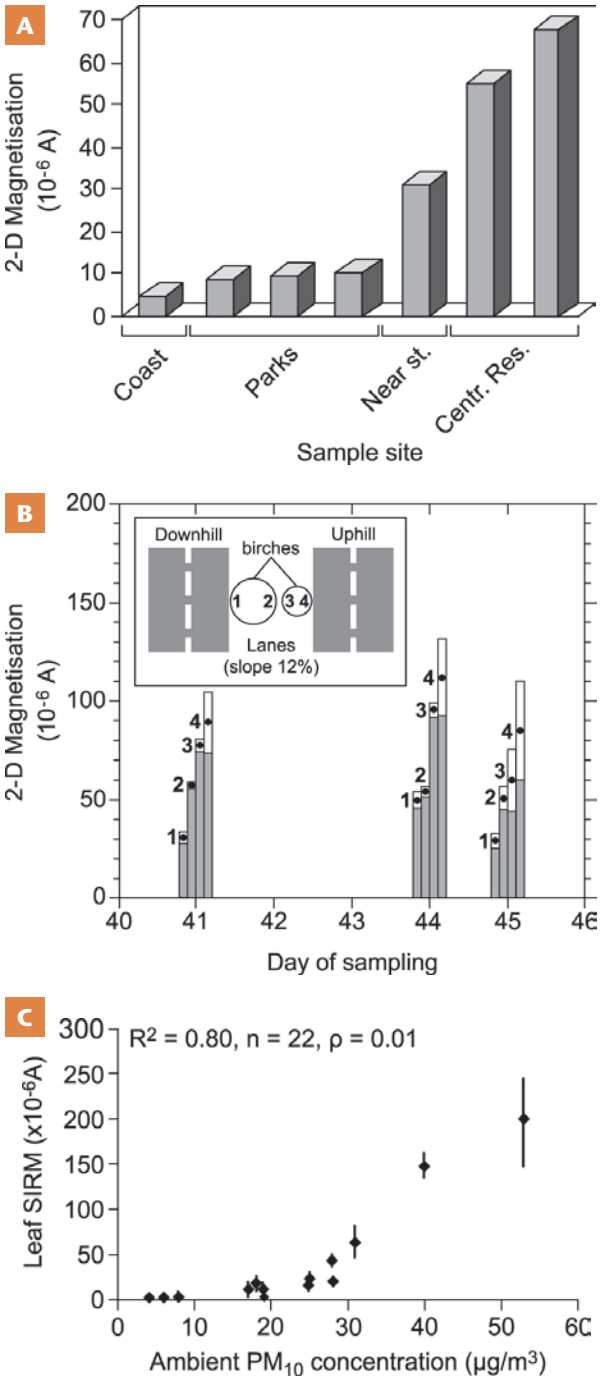

Figure 8 (**A**) Variation of birch tree leaf SIRMs (y-axis) with location and distance from roads ('Near st.' = near to street, 'Centr. Res.' = median strip, four-lane highway). (**B**) Variation of birch tree leaf SIRMs adjacent to the uphill and downhill lanes of a dual carriageway (four-lane highway). (**C**) Strong, direct correlation between leaf SIRMs and ambient PM_{10} concentrations. From Matzka and Maher (1999), Maher et al. (2008) and Mitchell and Maher (2009)

and cognitive development in children (Koller et al. 2004). Given the high correlation coefficients between SIRM, Pb and ambient PM_{10} concentrations, leaf SIRM measurements (made easily, rapidly and cheaply) appear valuable as a robust proxy predictor capable of providing unprecedentedly high spatial resolution data for assessment of human exposure to these damaging pollutants. Anyone can immediately reduce their exposure to vehicle pollution by walking on the downhill side of the road, where possible with intervening trees to act as a pollution 'filter'.

CONCLUSIONS

The environmental sensitivity of the magnetic minerals present in soils, sediments and dusts provides us with remarkable records of past changes in climate and of changes and health hazards in our urban environment. More than half the world's population depends on and is at risk from monsoonal rainfall; understanding how the monsoons have changed in the past is essential for predicting future changes. In our urban environments, the sensitivity and speed of magnetic measurements make biomagnetic monitoring of particulate pollution of potential utility all around the world.

ACKNOWLEDGMENTS

The author gratefully acknowledges financial support through a Royal Society Wolfson Research Merit Award.

REFERENCES

Aust A, Ball JC, Hu AA, Lighty JS, Smith KR, Straccia AM, Veranth JM, Young WC (2002) Particle characteristics responsible for effects on human lung epithelial cells. Research Report 110, Health Effects Institute, Boston, MA

Bealey WJ, McDonald AG, Nemitz E, Donovan R, Dragosits U, Duffy TR, Fowler D (2007) Estimating the reduction of urban PM_{10} concentrations by trees within an environmental information system for planners. Journal of Environmental Management 85**:** 44-58

Calderón-Garcidueñas L and 14 coauthors (2008) Long-term air pollution exposure is associated with neuroinflammation, an altered innate immune response, disruption of the blood-brain barrier, ultrafine particulate deposition, and accumulation of amyloid β-42 and α-synuclein in children and young adults. Toxicologic Pathology 36: 289-310

Chaparro MAE, Gogorza CSG, Chaparro MAE, Irurzun MA, Sinito AM (2006) Review of magnetism and heavy metal pollution studies of various environments in Argentina. Earth, Planets and Space 58: 1411-1422

Cohen AJ, Anderson HR, Ostro B, Pandey KD, Krzyzanowski M, Kuenzli N (2005) The global burden of disease due to outdoor air pollution. Journal of Toxicology and Environmental Health, Part A: Current Issues 68: 13-14, 1301-1307

Dankers PH (1978) Magnetic Properties of Dispersed Natural Iron Oxides of Known Grain Size. Unpublished PhD thesis, University of Utrecht

Donaldson K (2003) The biological effects of coarse and fine particulate matter. Occupational Environmental Medicine 60: 313-314

Filippelli GM, Laidlaw MAS, Latimer JC, Raftis R (2005) Urban lead poisoning and medical geology: An unfinished story. GSA Today 15(1): 4-11

Gautam P, Blaha U, Appel E (2005) Magnetic susceptibility of dust-loaded leaves as a proxy of traffic-related heavy metal pollution in Kathmandu city, Nepal. Atmospheric Environment 39: 2201-2211

Halsall CJ**,** Maher BA, Karloukovski VV, Shah P, Watkins SJ (2008) A novel approach to investigating indoor/outdoor pollution links: Combined magnetic and PAH measurements. Atmospheric Environment 42: 8902-8909

Heller F, Liu TS (1986) Palaeoclimatic and sedimentary history from magnetic susceptibility of loess in China. Geophysical Research Letters 13: 1169-1172

Kim W, Doh S-J, Park Y-H, Yun S-T (2007) Two-year magnetic monitoring in conjunction with geochemical and electron microscopic data of roadside dust in Seoul, Korea. Atmospheric Environment 41: 7627-7641

Koller K, Brown T, Spurgeon A, Levy L (2004) Recent developments in low-level lead exposure and intellectual impairment in children. Environment Health Perspectives 112: 987-994

Liu QS, Banerjee SK, Jackson MJ, Maher BA, Pan Y, Zhu R, Deng C, Chen F (2004) Grain sizes of susceptibility and anhysteretic remanent magnetization carriers in Chinese loess/paleosol sequences. Journal of Geophysical Research 109(B3): B03101, doi: 10.1029/2003JB002747

Maher BA (1988) Magnetic properties of some synthetic sub-micron magnetites. Geophysical Journal of the Royal Astronomical Society 94: 83-96

Maher BA (2008) Holocene variability of the East Asian summer monsoon from Chinese cave records: a re-assessment. The Holocene 18: 861-866

Maher BA, Thompson R (1992) Paleoclimatic significance of the mineral magnetic record of the Chinese loess and paleosols. Quaternary Research 37: 155-170

Maher BA, Thompson R (1995) Palaeorainfall reconstructions from pedogenic magnetic susceptibility variations in the Chinese loess and paleosols. Quaternary Research 44: 383-391

Maher BA, Thompson R, Zhou LP (1994) Spatial and temporal reconstructions of changes in the Asian palaeomonsoon: A new mineral magnetic approach. Earth and Planetary Science Letters 125: 461-471

Maher BA, Alekseev A, Alekseeva T (2002) Variation of soil magnetism across the Russian steppe: its significance for use of soil magnetism as a palaeorainfall proxy. Quaternary Science Reviews 21: 1571-1576

Maher BA, Moore C, Matzka J (2008) Spatial variation in vehicle-derived metal pollution identified by magnetic and elemental analysis of roadside tree leaves. Atmospheric Environment 42: 364-373

Matzka J, Maher BA (1999) Magnetic biomonitoring of roadside tree leaves: identification of spatial and temporal variations in vehicle-derived particulates. Atmospheric Environment 33: 4565-4569

Mitchell R, Maher BA (2009) Evaluation and application of biomagnetic monitoring of traffic-derived particulate pollution. Atmospheric Environment 43: 2095-2103

Morris WA, Versteeg JK, Bryant DW, Legzdins AE, McCarry BE, Marvin CH (1995) Preliminary comparisons between mutagenicity and magnetic susceptibility of respirable airborne particulates. Atmospheric Environment 29: 3441-3450

Muxworthy AR, Schmidbauer E, Petersen N (2002) Magnetic properties and Mössbauer spectra of urban atmospheric particulate matter: a case study from Munich, Germany. Geophysical Journal International 150: 558-570

Ning Y, Luo W, An Z (2008) A 130-ka reconstruction of precipitation on the Chinese Loess Plateau from organic carbon isotopes. Palaeogeography, Palaeoclimatology, Palaeoecology 270: 59-63

Özdemir Ö, Banerjee SK (1982) A preliminary magnetic study of soil samples from west-central Minnesota. Earth and Planetary Science Letters 59: 393-403

Özdemir Ö, Dunlop DJ, Moskowitz BM (1993) The effect of oxidation on the Verwey transition in magnetite. Geophysical Research Letters 20: 1671-1674

Pandey SK, Tripathi BD, Prajapati SK, Mishra VK, Upadhyaya AR, Rai PK, Sharma AP (2005) Magnetic properties of vehicle-derived particulates. Ambio 34: 645-646

Pope CA III, Burnett RT, Thun MJ, Calle EE, Krewski D, Ito K Thurston GD (2002) Lung cancer, cardiopulmonary mortality, and long-term exposure to fine particulate air pollution. Journal of the American Medical Association 287: 1132-1141

Porter SC, Hallet B, Wu X, An Z (2001) Dependence of near-surface magnetic susceptibility on dust accumulation rate and precipitation on the Chinese Loess Plateau. Quaternary Research 55: 271-283

Sartori M, Evans ME, Heller F, Tsatskin A, Han JM (2005) The last glacial/interglacial cycle at two sites in the Chinese Loess Plateau: Mineral magnetic, grain-size and ^{10}Be measurements and estimates of palaeoprecipitation. Palaeogeography, Palaeoclimatology, Palaeoecology 222: 145-160

Shu J, Dearing JA, Morse AP, Yu L, Yuan N (2001) Determining the sources of atmospheric particles in Shanghai, China, from magnetic and geochemical properties. Atmospheric Environment 35: 2615-2625

Szönyi M, Sagnotti L, Hirt AM (2008) A refined biomonitoring study of airborne particulate matter pollution in Rome, with magnetic measurements of *Quercus Ilex* tree leaves. Geophysical Journal International 173: 127-141